Failure Engineering Study and Accelerated Stress Test Results for the Mars Global Surveyor Spacecraft's Power Shunt Assemblies

Mark Gibbel
Jet Propulsion Laboratory
California Institute of Technology
mark.gibbel@jpl.nasa.gov

Timothy Larson
Jet Propulsion Laboratory
California Institute of Technology
timothy.w.larson@jpl.nasa.gov

ABSTRACT

An Engineering-of-Failure approach to designing and executing an accelerated product qualification test was performed to support a risk assessment of a "work-around" necessitated by an on-orbit failure of another piece of hardware on the Mars Global Surveyor spacecraft. The proposed work-around involved exceeding the previous qualification experience both in terms of extreme cold exposure level and in terms of demonstrated low cycle fatigue life for the power shunt assemblies.

An analysis was performed to identify potential failure sites, modes and associated failure mechanisms consistent with the new use conditions. A test was then designed and executed which accelerated the failure mechanisms identified by analysis. Verification of the resulting failure mechanism concluded the effort.

INTRODUCTION

This study and the associated accelerated stress tests were performed for the Mars Global Surveyor (MGS) spacecraft, which has recently completed the process of circularizing its orbit around Mars. During solar array deployment following launch, a damper failure caused structural damage to one solar array panel. This necessitated changing the aerobraking profile of the mission [Ref 1]. Consequently, the required mission re-plan involved subjecting the 22 power shunt assemblies (PSA's) to an additional eclipse season at Mars. The PSA's are small, low mass units that are located directly on the solar panels. See Figures 1 through 3. Compounding the situation is the fact that during this additional eclipse season the hardware will be subjected to eclipse periods 50% longer than originally planned. Consequently, some of the Partial Shunt Assemblies (PSA's) were predicted to reach –100°C during this added eclipse season rather than the previous limit of –50°C (flight acceptance test level). Moreover, the original flight mission required about 25,000 thermal cycles of magnitudes varying from about 10°C to 50°C. These cycles are associated with various spacecraft maneuvers during cruise, orbit insertion operations, and planetary orbital eclipses, among others. The variation in magnitude is driven by a large number of variables that are outside the scope of this paper. The new mission is complicated by the addition of more than 500 deep (around 100°C amplitude) thermal cycles after cruise and before mapping can be started.

During normal spacecraft operation all excess power is used to keep the batteries charged. When the batteries reach full charge the excess power is shunted into the PSA's. During mapping orbits, the spacecraft travels in and out of the planet's shadow. Power shunting occurs only during the last twenty or so sunlit minutes just prior to the start of a new eclipse. The PSA design itself is clever but simple, containing about 35 piece parts in all and is about 30 cm by 4 cm by 4 cm in size. See Figures 2 through 4.

The spacecraft's power regulation design is fault tolerant (degrades gracefully should individual PSA's fail). As such, the risk associated with a PSA failure is not considered high but it was deemed prudent to understand the risk and its likelihood by performing a 'delta qualification' test. Because time was of the essence, an accelerated qualification test was the only feasible option. The focus of this paper is on the methodology for designing and executing such a test.

A variety of analyses, simplified failure mechanism models, material property measurements and accelerated stress tests were performed to assess the likelihood of a PSA failure under the new in-flight cold exposures. Spare flight PSAs and some spare piece parts were used to perform an accelerated life test. One mission was estimated to be equivalent to approximately 1,500 to 1,800 cycles over the test temperature range of –125°C to +100°C. During

test, the PSAs were power cycled similar to their in-flight operation. Electrical testing and failure mechanism verification (failure analysis) waere performed after the accelerated qualification to assess the effects of the new mission environment on both performance and physical integrity.

Pre-test analysis indicated that bondwire tensile and shear fatigue at the die bond site and overstress of the bond or wire were the most likely failure mechanisms. Post-test analysis verified this expectation. One redundant bondwire in each of two different transistors were found to have zero pull strength after the test. However, none of the PSAs under test failed due the significant amount of redundancy (in the units and internal to the transistors). The MGS spacecraft has now successfully completed 2 years of flight, including the deep eclipse thermal cycles that necessitated this work to be performed. In-flight data and data analysis has indicated that minimum PSA temperature was about -92°C and that the largest cycle amplitude was 95°C. This is consistent with the design of the accelerated qualification test.

Test Hardware Description

Thermal cycle life testing was deemed prudent for the power shunting hardware. The spacecraft system used a complex shunting scheme that has redundancy at PSA unit level down to the driven transistor level. Spare flight PSAs and transistors were selected as the test vehicles. This hardware was originally manufactured in the early 1990's. Figures 2 through 4 show one of the test articles. The approximately 35 piece parts are all mounted directly to the metal chassis for good heat conduction (because of the space environment). One drive and five driven transistors are used. The current carrying driven transistors have 4 emitter wires and 2 base wires for redundancy. The entire load into a PSA can be handled by a single bondwire within a single driven transistor. The low-current drive transistors are not redundant at PSA unit level but the power system has redundancy through the use of multiple PSA units.

Transistors:

The transistors in the PSAs utilize a "stud mounted" packaging design (see Figures 4 and 5). The die is attached to a BeO substrate, which is attached to a post on the nickel-plated copper stud. The bondwires are made of 99.99% pure Al and are bonded to Al pads on the die and to gold plated nickel terminals at the post end. Their diameters are 0.010 inches in the driven transistors and 0.008 inches in the drive transistor. The bonds to the die and to the posts are ultrasonic wedge bonds as shown in a close-up photograph (Figure 6).

PRE -TEST ANALYSIS

Failure Mode/Mechanism Analysis

An analysis similar to a Failure Modes Effects and Critically Analysis (FMECA) was performed on the PSAs, except that, failure mechanism and failure mechanism model availability data was included. This analysis identified the need to perform several tests to verify the likelihood of occurrence of various failure mechanisms. This analysis was done to identify the most critical failure sites for monitoring and to identify the failure mechanisms that were to be accelerated during the testing. Failure modes considered were either: open, short, out of specification or drift. The five failure mechanisms associated with these failure modes were: 1) material fracture as a result of exposure to temperature extremes, 2) thermally induced fatigue of the packaging materials, 3) out of specification performance at the temperature extremes, 4) electrical hysteresis associated with repetitive thermal cycles and 5) aging. Opens and parameter drift (due to aging, radiation degradation, or temperature) were considered more likely than shorts given the fact that the most likely opportunity for shorting (i.e. launch), has passed with no failures observed[1]. However, opens (internal to the transistors) due to fracture (of the packaging materials: die, die attach, substrate, and substrate attach), were concluded to be not very likely based on special tests conducted as a part of this study. Consistent with the historical data of Reference (2), opens as a result of thermally induced fatigue of the transistor bondwires, were concluded to be the most probable failure mechanism. The accelerated stress/life test that Lockheed-Martin conducted during this study is considered to be the best method for assessing the likelihood of occurrence of these remaining failure mechanisms.

---

1 However, one credible way a short could be created would be to first fatigue a bond wire and when it breaks, it "springs back" making contact with an adjacent conductor.

Wirebond System Displacement and Fatigue

The bondwire system is subjected to stresses and strains over the course of a thermal cycle. These thermal cycles can be the result of a power cycle or an external cycle induced by the environment. Because the pure Al bondwire is far less stiff than the die or BeO substrate, the bondwire is constrained to the displacement of the substrate (in the plane of the substrate), until the bondwire fails. In a like manner, the die is constrained to the displacement of the BeO (minus some minor compliance in the thin gold eutectic die attach). The bondwires are also displaced a small amount perpendicular to the plane of the die via thermal expansion of the Nickel "A" post material.

Geometry Considerations

These bonds are unique in that the geometry is different than a classical ultrasonic wedge bond. In a typical wedge bond, the wire at the heel is significantly deformed (width is 2 to 3 times the initial wire diameter and thinned correspondingly). The tool used to form these bonds did not deform the wire any appreciable amount. See Figure 6. As a result one would expect the heels to be relatively strong. Moreover, the geometry of the base bondwires would result in significant moments being applied to the bond area parallel to the axis of the wire. As such, the bond area would undergo alternating tension and compression cycles. This could lead to fatigue failure of the bond material. Cracks would initiate in the higher stress areas of the bond perimeter and work inward. In a similar fashion, the emitter bondwires would be subjected to alternating tension and compression cycles in an axis perpendicular to the wire axis.

Reported Failure Types

Metallurgical fatigue failures have been reported in some bondwire systems where large diameter wires were subjected to the classical wedge bonding. These were open cavity power devices. The failures occurred after being subjected to a relatively small number of power cycles [Harman 1997]. Wire flexure fatigue has been reported to be a relevant failure mechanism for heel failures [Phillips 1974]. Shear fatigue failures between the bond pad and substrate have been shown to be associated with shear fatigue [Pecht 1989]. The above failure mechanisms and relevant models have been summarized by [Lall, Pecht Hakim 1997].

For ball and wedge bonds, a heel failure (particularly at the die end) has been reported as the most likely failure site [Lall, Pecht and Hakim 1977]. However, no reported data was found regarding failure of the bond metal.

Related Investigations

Several material properties of interest were not found the open literature or other federal laboratories or university databases available for this study. In these cases, special tests were performed to measure the needed properties or to bound their effect. Other tests were also performed to rule out various failure mechanisms. For example failures associated with the fracture toughness of very thick (0.7 inches) BeO at high temperatures has been reported in the literature. Unfortunately, no data could be found for the temperature range of interest or for sizes relevant to electronic packaging. Although not reported in detail in this paper, separate testing was performed and concluded that this failure mechanism was not an issue for the planned mission. A mechanical over stress test of the transistor packaging materials was also performed. This was done by subjecting one PSA to an extreme thermal cycle range of –145°C to +100°C for 1 cycle followed by 24 cycles from –125°C to +100°C. No failures were detected during this overstress testing, thereby allowing over stress associated with the colder exposure to be deemed unlikely for this investigation. Table 2 summarizes the material properties used in this study and documents their source.

EXPERIMENTAL DESIGN

Three spare drive transistors and three spare PSAs were used as test articles. All devices were from the same lot codes as the hardware used in the spacecraft. The PSAs were electrically active and operated at the same power levels as in flight. They were instrumented such that the loss of a single transistor could be detected. Internal redundancy of the transistor bondwires (and the desire to preserve the integrity of the PSA packaging), eliminated the ability to detect the failure of an individual bondwire during the test. The test set (fixture, chamber and test articles) was also instrumented with temperature sensors. The test articles were cycled in a dry gaseous nitrogen environment from -125°C to +100°C for 2,000 cycles.

For the purposes of estimating an acceleration factor for designing the test, the acceleration factor (AF) was considered

proportional to the strain in the bondwire:

$AF = (\delta 1/\delta 2)^m$

Where $\delta 1$ and $\delta 2$ are the strain ranges associated with a test cycle and a flight cycle, respectively. Additionally, m is the plastic Coffin-Manson exponent.

Measurements of the geometry from recently built transistors were made. Strains were estimated by incorporating this geometric data and the material property data of Table 1 into a spreadsheet-based model. This model included the various coefficients of thermal expansion as a function temperature. Note that as the lower temperature drops (i.e. gets colder), the difference in the material CTE decreases. Said another way, less CTE induced damage is accumulated as the lower test temperature is decreased. Because no explicit value for the plastic Coffin-Manson exponent for 99.99% pure Aluminum could be found, the analysis used the value published for 2224 T351 Aluminum of 1.7 [S. Suresh 1991] and a second value of 1.5. This lower second value was used to account for the uncertainty in the plastic Coffin-Manson exponent for 99.99% pure Aluminum. If the higher value were to be the true value, then using this lower value to calculate the required number of test cycles would result in about 40% margin on the number of test cycles required. The results of these calculations are summarized in Table 1.

Bondwire integrity was assessed after testing by comparing bondwire pull test strengths to that of control samples that hadn't undergone the temperature cycling. Verification of the failure mechanism that resulted in the degradation of bondwire pull strength was performed by viewing the failure sites with the aide of a Scanning Electron Microscope (SEM). In all, 22 bondwires (6 in three driven and 4 in two drive transistors) were used as control samples. The bondwires from the driven transistors were from the same lot date codes as the test articles and the flight devices. The drive transistors used as control samples were from a current lot due to unavailability of flight spares.

Based on this, acceleration factors for a test cycle (–125°C to +100°C) were estimated. These ranged from about 2 (for a 160°C amplitude test cycle and m equal to 1.5) to 230 (for a 10°C amplitude mission cycle and m equal to 1.7).

RESULTS

No failures of a PSA or of individual transistors occurred during the temperature cycling.

The SEM photograph shown in Figure 7 indicates that the primary bonding area was at the heel and toe, with some minor bonding around the perimeter. Moreover, the SEM photograph in Figure 8 confirms that fatigue of the bond was the life limiting failure mechanism.

The distributions of pull strengths, failure categories and powered/temperature cycling conditions are shown in Table3. For the control devices, the failure category distributions were heel at die (59%), failure in bond at die (27%), and midspan wire failure (14%). However, for the wirebonds subjected to thermal cycling (via power cycling or chamber excursions or both), 97% failed in the bond at the die (interface between the wire and metalization at the die). The dominant failure category for the control devices was consistent with the literature (i.e. heel failure at die most likely) [Lall, Pecht, Hakim, 97, Harman 74, 97]. However, for the cycled bonds, the dominant failure category (bond failure) is quite different than what would be expected based on the literature.

Note that in the control samples, the base bondwires were slightly weaker than the emitter bondwires. Assuming that, on average, the tested bondwires had the same pull strength at the start of the test as the control bondwires, then the base bondwires have less than 20% of their initial strength left at the end of the accelerated life test. Conversely, the emitter bondwires had about 30% of their initial strength left. Also, on average, the base and emitter bondwire pull strength degraded by 264 and 295 grams, respectively. Based on this, the initial bondwire pull strength would need to be significantly greater than specified by the Military Standard 883C for wires of these diameters (80 grams for the driven transistor bondwires, 50 Grams for the drive transistors).

CONCLUSIONS

Some uncertainty remains regarding the actual acceleration factors for the life test, based on uncertainties in the Coffin-Manson exponent for 99.99% Aluminum and the types of failures seen after the pull tests. Special tests to measure the Coffin-Manson exponent could be performed. Coupled with this measurement, a

finite element model of the wire bond system could be used to confirm the acceleration factors. It is hypothesized that the flexure fatigue model presented in [Lall, Pecht Hakim 1997] may apply to the failure mechanisms observed here. However, additional study would be required to confirm this.

Although this type of wire bond was found to only bond around the perimeter they appear to have superior heel strength (when compared to conventional wedge bonds) and sufficient life for the MGS mission which included extensive thermal cycling.

The dominant failure mechanism found in these wirebonds was fatigue of the bond metalization, rather than the more common case of bondwire fatigue at the heel of the bond.

Mil Std 883C values for minimum bondwire pull test strengths are not necessarily a good guideline when the use environment involves either thermal or power cycling.

ACKNOWLEDGEMENTS

The authors wish to acknowledge the help provided by the following individuals: Ray Zercher and Richard Lesnick of Lockheed Martin Astronautics for their work in designing the test set and for conducting the thermal cycle testing; Gary Plette of JPL for his work in measuring the CTE of BeO; Steve Freiman, Chief, Ceramics Division NIST for providing sources of material property data; Jim Okuno and Ken Evans of the JPL Failure Analysis Lab for the pull tests and SEM work; James Kulleck of the JPL Thermal and Propulsion Section for additional SEM investigations; George Harman, of NIST and Henning Liedecker from the Goddard Space Flight Center for their generous provision of time and guidance.

The work described in this paper was conducted at the Jet Propulsion Laboratory, California Institute of Technology, and Lockheed Martin Astronautics under a contract with the National Aeronautics and Space Administration. The failure mechanism investigation in this work was partially funded by the NASA Code Q sponsored Failure Detection and Prevention Program.

REFERENCES

Aviation Week and Space Technology, November 17, 1997.

Lall, Pecht, Hakim, "Influence of Temperature on Microelectronics", 1997, CRC Press, ISBN 0-8493-9450-3.

Military Standard 883C, Notice 4, Method 2011.5, Test Condition 3.1.3, Dated 29 November 1985.

S. Suresh, "Fatigue of Materials", Cambridge Press, 1991, Page 138.

Harman, "Wire Bonding in Microelectronics Materials, Processes, Reliability and Yield", Mc GrawHill, 1997, ISBN 0-007-032619-3.

Harman, G.G. "Metallurgical Failure Modes of Wire Bonds", 12th International Reliability Physics Symposium, 1974.

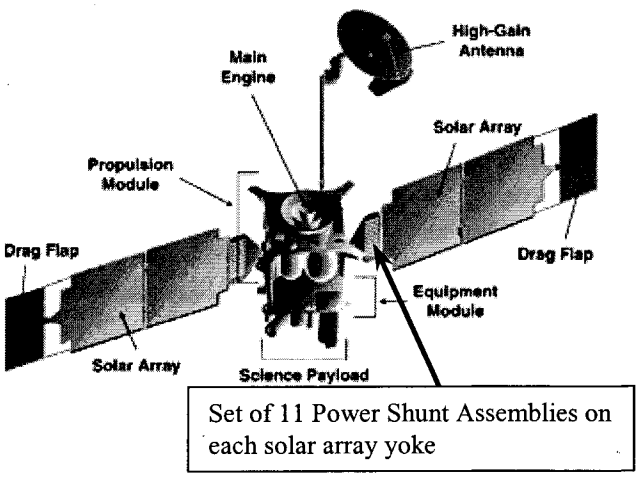

Figure 1. Overview of MGS spacecraft showing location of power shunt assemblies (PSA).

Mission Phase	Cycles	TEMPERATURE RANGE			Total strain in wire	Estimated Acceleration Factor (AF)		Equivelent Test Cycles	
		T1	T2	dT		Fatigue exponent = 1.5	Fatigue exponent =1.7	1.5	1.7
Acceptance Test	18	100	-60	160	0.0031	1.9	2.1	9.4	8.6
T/V from	16	70	-55	125	0.0024	2.8	3.2	5.8	5.1
Cruise	4700			57	0.0011	9.0	12.0	523.2	390.4
Minimum thermal cycle	1			10	0.0002	122.3	232.0	0.0	0.0
Pre-Eclipse ANS Cycling (every 100 min from 9/11 to 1/2)	1627	20	-10	30	0.0006	23.5	35.8	69.2	45.4
Pre-Eclipse AB Drag Pass (P-0 to P-90)	90	20	-50	70	0.0014	6.6	8.5	13.6	10.6
Phase 1 Eclipse Season ANS Cycling (Every 100 Min from 1/2 to 4/1)	1280	20	-10	30	0.0006	23.5	35.8	54.4	35.7
Phase 1 Eclipse Season Eclipse & AB Drag Pass (1/2 to 4/1)(60 min eclipse)(P-90 to P-300)	210	-40	-100	60	0.0010	10.8	14.9	19.4	14.1
Additional eclipse cycles due to mission replan	500			100	0.0019	3.9	4.6	129.3	108.0
Science ANS Cycling (4/1 to 11/1/98)(100 min spin)	3080	20	-10	30	0.0006	23.5	35.8	130.9	85.9
SCI(4/1 to 11/1/98)(6 hr orbit)(60 min Off-Point)	856	20	-70	90	0.0017	4.5	5.5	189.1	154.6
Eclipses during Science (4/1 to 11/1/98)(Avg 30 min)	856	20	-50	70	0.0014	6.6	8.5	129.7	100.8
Phase 2 ANS Cycling (11/1 to 4/1/99)(100 min spin)	2174	20	-10	30	0.0006	23.5	35.8	92.4	60.6
Phase 2 AB/Eclipse (11/1 to 4/1/99)(P-301 to P-900)	600	20	-70	90	0.0017	4.5	5.5	132.5	108.3
Mapping 1 Mars yr =687 days 40 Min Eclipses 12 orbits per day	8760	20	-50	70	0.0014	6.6	8.5	1,327.1	1,031.9
Relay phase 3 Earth years	0	20	-50	70	0.0014	6.6	8.5	0.0	0.0
Totals	**24,768**							**1,871**	**1,456**

NOTE: Assumes a 10C rise from thermal control surface to bondwire pad at hot and off (I.e. battery operation) cold

Table 1. Estimate of mission exposures and test accelerations and equivalent test cycles.

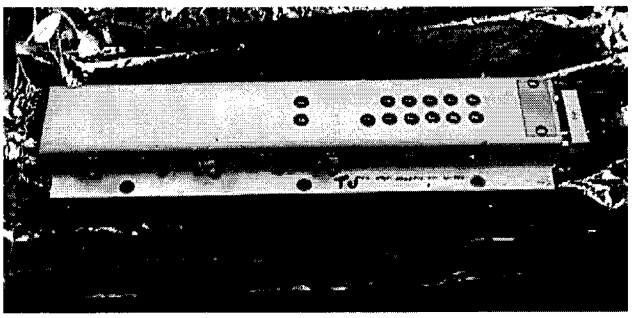

Figure 2. Overview of Power Sunt Assemblies, looking from outside.

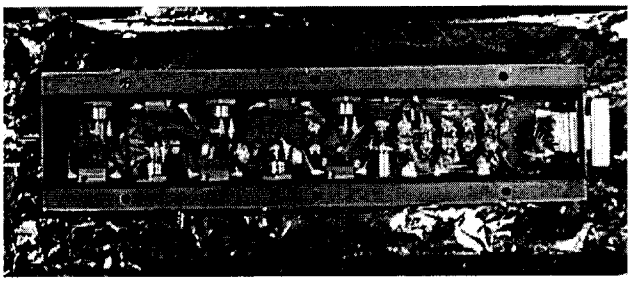

Figure 3. Overview of Power Shunt Assembly looking inside.

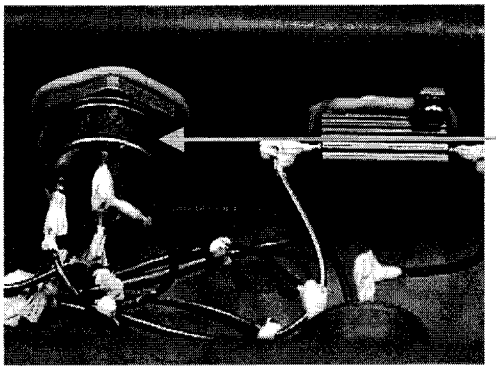

Close-up of driven transistor bonded to sheet metal housing. Note all external wire interconnects are coated with a dielectric (white material)

Figure. 4. Close-up of a driven transistor bonded to side of housing.

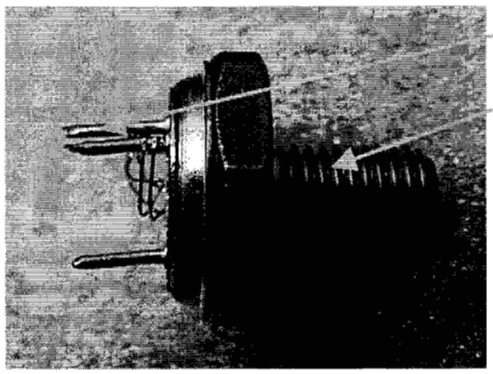

Figure 5. Close-up of a de-lidded driven transistor.

MATERIAL	PROPERITY	VALUE	UNITS	SOURCE	COMMENT
Aluminum	CTE -125 to -75C -75 to 100C	 18 23	PPM/C	Thermo-physical Properties of Matter (TPOM)	
	Paris power law Exponent	1.5 to 1.7	---	Aerospace data	
BeO	CTE -125 to -75C -75 to 50C 50 to 100C	 1.8 3.7	PPM/C	 Test Test TPOM	Test performed by JPL's Analytical Chemistry Group
	Fracture Toughness	?	joules		➢ Toughness Unknown but verified by test to be greater than that associated with cycling a specimen between room temperature and LN2 via "dunking"
Copper	CTE -125 to -75C -75 to 100C	 13 17	PPM/C	--- TPOM TPOM	
	Modulus of Rupture	---	---	---	
	Paris power law Exponent	2	---	Aerospace data	

Table 2. Summary of material properties used the stress analyses.

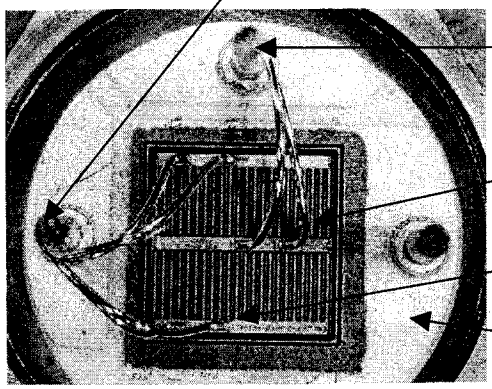

Figure 6. Top view of Transistors showing bondwire configurations. Bondwires are dead soft Aluminum 0.010 inches in Diameter on Aluminum metalization. Posts are Nickle. All are bonds ultrasonic. Bonds to die are orthodyne bonds while bonds to post are wedge bonds.

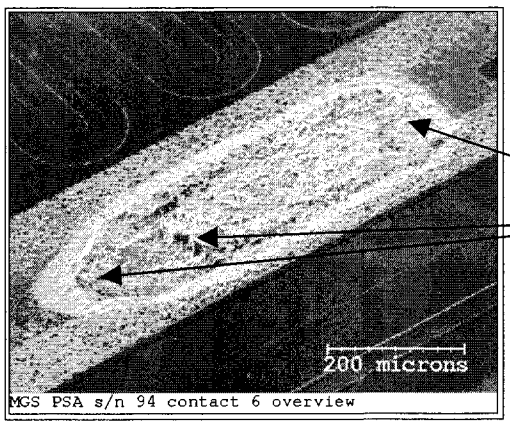

Figure 7. View of bond pad #6 in S/N 094 showing area where bonding occurred.

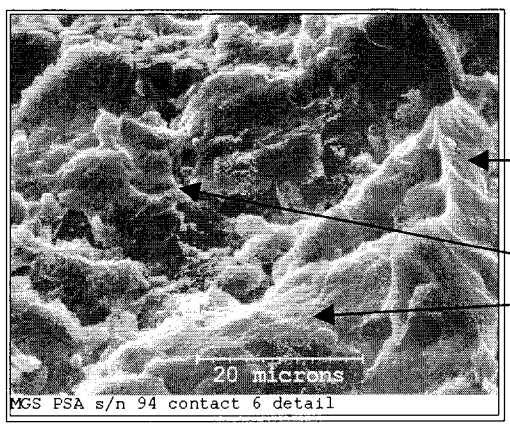

Figure 8. Close up of region shown by middle arrow in Figure XXX.

Bondwire Pull Test Results All Driven Transistors from same with lot date codes of 9049																	
	Pull Strength (grams)						Location of Failure Site (blank= failure in wire at die bond location)						Thernal Cycle	Power Cycle	Control Sample	Type of Device	Notes
S/N	1	2	3	4	5	6	1	2	3	4	5	6					
71	216	371	360	337	511	425			Die Heel	Die Heel	Midspan	Die Heel			x	Driven	
81	410	386	397	419	489	386			Die heel	Die Heel	Midspan	Die Heel			x	Driven	
119	273	263	416	460	439	456			Die Heel	Die Heel	Midspan	Die Heel			x	Driven	1
80	18	21	318	200	0	NR							x			Driven	
91	16	62	58	175	93	86							x			Driven	
155	50	67	175	167	310	67							x			Driven	1
83	19	16	210	227	53	40							x	x		Driven	
94	15	15	155	86	59	219							x	x		Driven	
121	91	165	153 *	158	23	NR			Post Heel				x	x		Driven	
143	78	207	282	289	145	331							x	x		Driven	
151	38	33	24	186	0	19							x	x		Driven	
191	31	52	171	208	24	100							x	x		Driven	
193	33	81	65	113	19	81							x	x		Driven	1
194	73	57	107	153	137	105							x	x		Driven	
1	410	411	--	--	--	--	Die Heel	Die Heel	--	--	--	--			x	Drive	2
2	507	402	--	--	--	--	Die Heel	Die Heel	--	--	--	--			x	Drive	2
167	165	189	--	--	--	--			--	--	--	--	x	x		Drive	

Notes: NR = not recorded

1) Original FA performed at LM wiring convention not detailed beyond emitter side side and base.
2) These devices were from current manufacturer's lot due to lack of spares of original flight parts.

Table 3. Summary of failure analysis results (pull strengths and failure location).